Nonlinear gyrokinetic simulation of saturated turbulence produced by fast ion precession driven drift instability in reversed shear plasmas

B. J. Kang, C. Angioni, T. S. Hahm

Abstract

Transport caused by a fast ion precession driven drift instability in reversed shear plasmas [B. J. Kang and T. S. Hahm, Physics of Plasmas 26, 042501 (2019)] is investigated from nonlinear gyrokinetic simulation using the GKW code. Nonlinearly saturated spectrum of fluctuation intensity decays as k_θ^{-3} and considerable transport rate roughly with the level of gyroBohm diffusivity is observed for fast ions.

Keywords: Fast ion driven instability, gyrokinetic simulation

1. Introduction

Predicting turbulence and transport in burning plasmas in the presence of fusion product α-particles is one of outstanding research subjects in magnetic fusion energy community. Reversed shear (RS) plasma is known for good confinement [1, 2, 3] and one of the leading advanced operation scenarios for a tokamak reactor. Alfvénic instabilities driven by α-particles in burning plasmas have been extensively studied as reviewed [4]. On the other hand, most studies on micriturbulence to date have focused on the transport of high energy fusion products due to the well-known instabilities including the ion temperature gradient (ITG) mode [5, 6] and the collisionless trapped electron mode (CTEM) [7]. In addition, the influence of α-particles on mean poloidal flow [8] and turbulence-driven zonal flows [9] has been investigated.

More recently, a new electron drift instability driven by the precession resonance with the high energy trapped ions in RS plasmas has been theo-

Email address: tshahm@snu.ac.kr (T. S. Hahm)

retically predicted [10] and identified from linear gyrokinetic simulations [11]. Possible influence of this new instability on transport of energetic ions is of high theoretical interest.

In this paper, we study nonlinear behavior of the new instability including turbulence spectrum at nonlinear saturation and heat transport of energetic ions (α-particles) and working gas (D and T ions), using the nonlinear gyrokinetic code, GKW [12] in the flux-tube toroidal geometry. The principal results are as follows :
i) Nonlinear saturation of fluctuation intensity is observed. Its k_θ-spectrum decays as k_θ^{-3}.
ii) Considerable heat transport rate roughly with the level of gyroBohm diffusivity is observed for fast ions. While D and T heat transport exhibits steady state values after the fluctuation intensity saturation, α-particle heat transport evolves slowly in time well after the intensity saturation.

2. Theoretical Model

We briefly summarize the theoretical model based on previous studies on the new instability. Our analytical local study of the instability [10] is based on the gyrokinetic equations in general toroidal geometry [13, 14]. Each species' dynamics is described by linearized electrostatic gyrokinetic equation with appropriate approximations respectively. We assume an adiabatic electron response and a fluid ion approximation for the main ions for $k_\parallel \mathrm{v}_{th,i} \ll \omega \sim \omega_{*e} \ll k_\parallel \mathrm{v}_{th,e}$ and $k_\perp \rho_i \ll 1$. Here, $\mathrm{v}_{th,j} = \sqrt{T_j/m_j}$ is the thermal speed of species j, ω is the mode frequency and $\omega_{*e} = \frac{k_\theta \rho_s C_s}{L_{ne}}$ is the electron diamagnetic frequency where $C_s = \sqrt{T_e/M_i}$, $\rho_s = \frac{cM_iC_s}{|e|B}$ and $L_{ne} = -\left(\frac{1}{n_e}\frac{dn_e}{dr}\right)^{-1}$. For $\omega/\omega_{bf} \ll 1$, fast ions are described by the bounce-averaged gyrokinetic equation [15, 16] where $\omega_{bf} = \frac{\epsilon^{1/2}\mathrm{v}_{th,f}}{qR}$ is the bounce frequency of fast ions. Even when usual ion temperature gradient (ITG) mode and collisionless trapped electron mode (CTEM) are stable, the resonant interaction between the electron drift wave and the reversed toroidal precession of trapped fast ions can lead to the new instability. Here, toroidal precession means the orbit-averaged toroidal drift of guiding centers in axisymmetric geometry. Trapped particles' toroidal precession motion can resonate with the drift wave and excite instabilities when trapped particles' precession motion is in the same direction as the drift wave's toroidal phase velocity. In RS

plasmas many fast ions reverse their toroidal precession direction and they can resonate with the electron drift wave. The energetic particle (EP) precession with electron drift wave for this new instability in RS plasmas plays a role which is very similar to the trapped electron precession resonance for CTEM in positive shear plasmas.

Then we can calculate the perturbed density responses of each species and derive a dispersion relation from the quasi-neutrality equation $\delta n_e = \delta n_i + Z_f \delta n_f$. By solving the dispersion relation for $\omega_r \gg \gamma$, the linear growth rate of the new instability can be calculated. The details are shown in Eqs. (5) - (12) of Ref. [10]. It has been shown that the new instability occurs when the fast ion temperature profile is more peaked than the density profile i.e., when $\frac{L_{nf}}{L_{Tf}}$ exceeds a critical value which approximately equals to 2/3 assuming that the equilibrium distribution function of fast ions is Maxwellian.

Furthermore, we have derived the nonlocal eigenmode equation in ballooning coordinate to address linear toroidal mode coupling [11]. Using the WKB method to find solutions of the eigenmode equation, the mode frequency and the linear growth rate as functions of various parameters are calculated and the results are well explained by the theoretical predictions. These results are shown in Figs. 3 - 7 of Ref. [11]. In addition, we have identified the new instability from the GKW gyrokinetic simulations in flux-tube toroidal geometry. Linearly unstable modes have been found for parameters for which the new instability is predicted from the local analytic theory [10]. Most of the simulation results are broadly consistent with the theoretical predictions. (Results and discussion are shown in Sec. IV of Ref. [11].)

In Ref. [10], the quasi-linear particle fluxes of each particle species were calculated from Eq. (36) to Eq. (39). However, there was a sign error in the expression for the quasi-linear paticle flux as explained in detail in the Appendix.

With this background, we perform a nonlinear gyrokinetic simulation using the GKW code in its nonlinear flux-tube version. In the electrostatic limit, GKW solves the following nonlinear toroidal gyrokinetic Vlasov equations as [12]

$$\frac{\partial \delta f}{\partial t} + \frac{c\mathbf{b} \times \nabla \langle \delta \phi \rangle}{B} \cdot \nabla \delta f \tag{1}$$
$$+(\mathrm{v}_\parallel \mathbf{b} + \mathrm{v}_\mathbf{D}) \cdot \nabla \delta f - \frac{\mathbf{b}}{m} \cdot (\mu \nabla B_0) \frac{\partial \delta f}{\partial \mathrm{v}_\parallel} = S$$

where $\mathbf{v_D}$ is the velocity of drift motion due to the inhomogeneous magnetic field. S is given by

$$S = -\left(\frac{c\mathbf{b}\times\nabla\langle\delta\phi\rangle}{B} + \mathrm{v}_{\mathbf{D}}\right)\cdot\nabla_p F_0 \\ +(\mathrm{v}_\parallel\mathbf{b}+\mathrm{v}_{\mathbf{D}})\cdot Z|e|\nabla\langle\delta\phi\rangle\frac{\partial F_0}{\partial E} \tag{2}$$

A derivation of Eqs. (1) and (2) from the modern nonlinear gyrokinetic equation [13] can be found in the Appendix of Ref. [7]. In particular, the parallel velocity space nonlinearity has been ignored and isotropic F_0 in velocity space has been assumed. In Eqs. (1) and (2), δf and F_0 are the perturbed and equilibrium distribution function respectively. Z is the charge number and $|e|$ is the elementary charge, $\mathrm{v}_\parallel$ is the parallel velocity, $\mathbf{b}$ is the unit vector aligned with equilibrium magnetic field, μ is the magnetic moment, $E = \frac{1}{2}m\mathrm{v}_\parallel^2+\mu B$ and $\delta\phi$ is the perturbed potential. The bracket $\langle ...\rangle$ indicates the gyro-phase average and ∇_p means that derivatives are taken at fixed E. In the present simulation, Eq. (1) is solved self-consistently ignoring the neoclassical transport term "$\mathbf{v_D}\cdot\nabla_\mathbf{p}F_0$" with the corresponding gyrokinetic Poisson equation in Fourier space assuming F_0 is a Maxwellian distribution function.

$$\sum_{sp} Z_{sp}n_{Rsp}\left[2\pi B\int d\mathrm{v}_\parallel d\mu J_0(k_\perp\rho_{sp})\hat{\delta f}_{sp} + \frac{Z_{sp}}{T_{Rsp}}\{\Gamma_0(b_{sp})-1\}\hat{\phi}\right] = 0 \tag{3}$$

where sp refers to the species of particles, $\hat{\delta f}$ indicates the Fourier representation of the perturbed distribution, $\Gamma_0(b_{sp}) = I_0(b_{sp})e^{-b_{sp}}$, I_0 is the modified Bessel function and $b_{sp} = k_\perp^2\rho_{sp}^2$. Finally, the electron response is assumed to be adiabatic.

3. Nonlinear gyrokinetic simulations

We have performed a nonlinear simulation using the GKW code [12]. GKW is a Vlasov code and we have adopted the flux-tube geometry. It can include various physics such as kinetic electrons, electromagnetic effects, collision, full general geometry and multi-species ions.

The nonlinear simulation parameters are almost the same as those of linear simulations [11]. We consider a collisionless plasma in tokamak cross

section geometry. Plasmas consist of electrons, D-T ions with $n_D = n_T$ and α particles. We take $r/a = 0.5$, $R/a = 3$, $q = 1.4$, $\hat{s} = -1$, $T_i/T_e = 0.1$, $T_f/T_e = 10$, $R/L_{Te} = R/L_{Ti} = 1$, $R/L_{Tf} = 30$, $R/L_n = 3$ and $n_f/n_e = 0.1$. Here we explore the possibility of turbulence that develops from this fast particle driven instability, what justifies the need of adopting somewhat academic parameters in order to remove the drive from the background (bulk plasma) species. (Of course this leads to unrealistic conditions, but)This allows us to investigate the existence and properties of this turbulence in a more specific manner and to provide a proof of principle of the existence and sustainment of this turbulence.

Equilibrium distribution function of all species is assumed to be Maxwellian. As mentioned before, main ions and α particles are described by the electrostatic nonlinear gyrokinetic equation while the electron response is adiabatic for simplicity and consistency with the analytic theory model. Furthermore, a cold main ion temperature with $T_i/T_e = 0.1$ which is favorable for studies of the new instability is chosen despite the fact that it is unrealistic for burning plasma experiments [17]. In addition, weak temperature gradients $R/L_{Ti} = R/L_{Te} = 1$ are used for our studies of the new instability in the absence of ITG and CTEM. We use 30 grid points in one turn along the field line. Velocity space is discretized over 64 points in the parallel velocity and magnetic moment is discretized over 32 points wth 43 toroidal modes and 339 radial modes where $(k_\theta \rho_s)_{max} = 2.50$, $(k_\theta \rho_s)_{min} = 0.0595$, $|k_r \rho_s|_{max} = 10.6067$ and $|k_r \rho_s|_{min} = 0.062762$. A natural question may arise as to the stability of reversed shear Alfvén eigenmode (RSAE) [18, 19] for the conditions we are considering. However, addressing this would require an electromagnetic global simulations with proper $q(r)$ profile near q_{min} which are beyond the scope of this letter.

Simulation results exhibit a nonlinear saturation of fluctuation amplitude after a brief linear growth phase as shown in Fig. 1. Long wavelength modes are prominent in both linear and nonlinear phases. The dominant mode in nonlinear phase is $k_\theta \rho_s = 0.1263$. Corresponding relative fluctuation amplitude is on the order of 10^{-2}. On the other hand, the most unstable mode in linear phase with the maximum linear growth rate is $k_\theta \rho_s = 0.2525$ in agreement with Ref. [11]. This indicates nonlinear spectral transfer towards longer wavelength modes. Fig. 2 shows the time averaged electrostatic potential summed over k_r. Saturated spectrum from GKW simulation exhibiting the intensity decaying as k_θ^{-3} from its peak at low k_θ is similar to analytic prediction (red dotted line), based on main ion Compton scattering

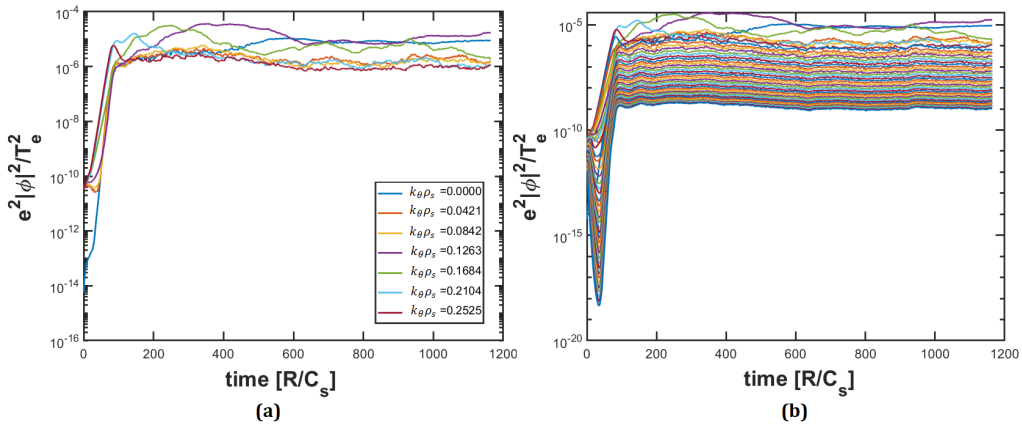

Figure 1: The time evolution of perturbed electrostatic potential from nonlinear GKW simulations. (a) shows 7 dominant modes and (b) shows all modes. Legend of (b) is omitted to avoid mess.

for CTEM [20]. This is also similar to the spectrum of CTEM obtained from nonlinear GKW simulations [7].

Ion Compton scattering transfers fluctuation energy to longer wavelength mode via Landau damping of nonlinearly generated beat wave (a virtual sound wave) on thermal ions [21]. Note that most fluid-like ions respond to the unstable modes with high phase velocity ($v_{th,i} \ll \omega/k_\parallel$), but can interact resonantly with low phase velocity virtual sound wave ($v_{th,i} \sim \omega''/k_\parallel''$). This observation suggests that the main ion Compton scattering is the prime candidate for main nonlinear saturation mechanism of the fluctuation intensity.

Figs. 3-(a) and (b) show the time evolution of particle fluxes and heat fluxes. Here, normalized Larmor radius ρ_* is defined as $\rho_* \equiv \rho_s/a$. Particle fluxes of all ion species show saturation after $t_N = R/C_s = 600$. Particle flux of main ions is outward while that of fast ions is inward. This is consistent with the theoretical prediction based on assumption of adiabatic electron response. On the other hand, heat fluxes show richer behavior. Heat flux of main ions show saturation after $t_N = 600$ and its direction is outward afterward while the direction of heat flux of fast ions varies in time. It becomes eventually outward at the end of the nonlinear simulation as one might expect, but without reaching a clear saturated state. We note that temperature profiles are fixed in time in our gradient driven simulation in flux-tube geometry.

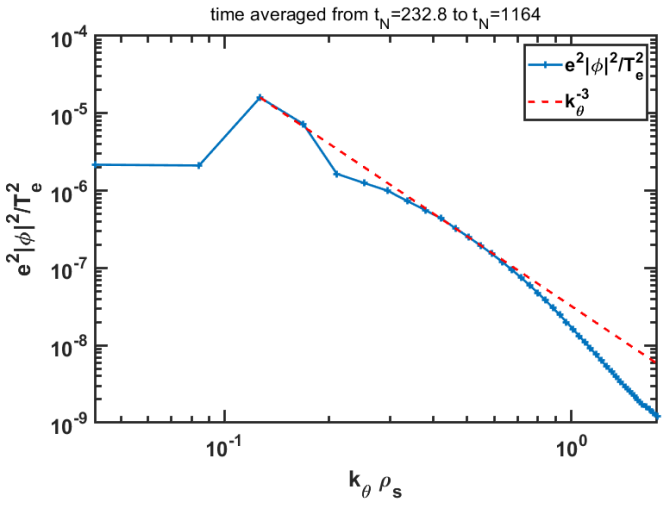

Figure 2: Time averaged perturbed electrostatic potential summed over k_r

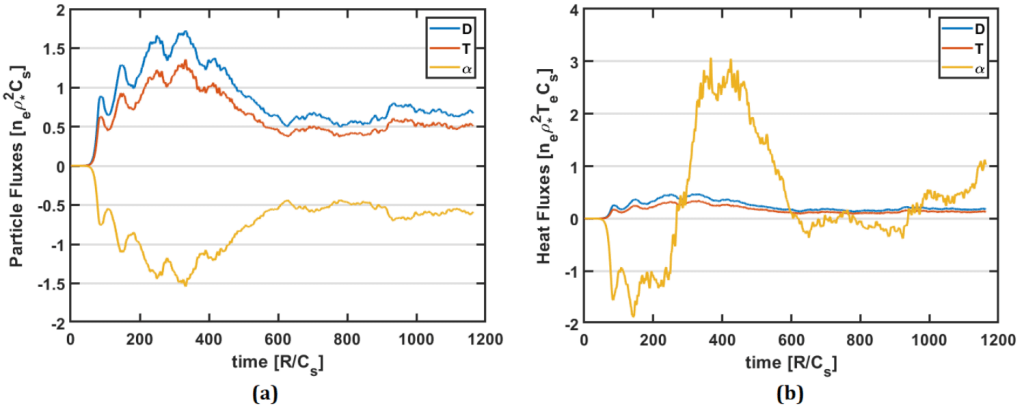

Figure 3: The time evolution of (a) particle fluxes, (b) heat fluxes and (c) the effective heat diffusivities from nonlinear GKW simulations. Here, $\chi_{GB} \equiv \rho_s^2 C_s/a$.

This temporal variation of fast ion heat flux suggests that even after nonlinear saturation of fluctuation amplitude and spectra presumably governed by the main ion nonlinearity, nonlinear interaction between the modes and fast ions ensues in a dynamical manner. Furthermore, since this temporal variation is observed only for heat flux involving energy moment of the perturbed distribution, not for the particle flux, the responsible mechanism should be kinetic in its nature.

It is interesting to note that some theoretical works based on phase space coherent structures lead to a prediction of finite time delay between the instantaneous turbulent heat flux and the steady state heat flux due to ITG turbulence [22]. This can be extended to our new instability driven α particle heat flux including the phase space granulation due to trapped tion precession resonance [23]. Comprehensive phase space diagnostics and analyses on nonlinear simulation data are desirable for further understanding, but beyond the scope of this paper.

As shown in Fig. 3-(b), the heat flux of α particle is much greater in magnitude in comparison to those of main ions. This is probably due to a very high value of $R/L_{T\alpha}$ (which drives the turbulence) used in simulations. If we define the effective thermal diffusivity of α particles as $Q_\alpha = -n_\alpha \chi_{eff,\alpha} \frac{\partial T_\alpha}{\partial r}$, we find $\chi_{eff,\alpha}$ is on the order of $10^{-1}\chi_{GB}$ (GyroBohm diffusivity using electron temperature). Since main ion heat flux is also carried by the turbulence which is driven by $\frac{\partial T_\alpha}{\partial r}$ (rather than weak $\frac{\partial T_D}{\partial r}$ or $\frac{\partial T_T}{\partial r}$), characterizing this off-diagonal flux with the effective diffusivity would end up misleading (with large values on the order of $10\chi_{GB}$). From Fig. 3, we observe that both particle and heat flux of D are greater than those of T considerably. For the linearly most unstable mode at $k_\theta \rho_s = 0.2525$, $k_\theta \rho_D = 0.08$ and $k_\theta \rho_T = 0.10$ for thermal working ions due to $T_e/T_i = 10$. Therefore, the difference in the flux is not due to the finite orbit width effects which should be negligible. Furthermore, the phase velocity of that most unstable mode is $\omega/k_\parallel \simeq \omega q R \simeq 1.2 C_s$ which is much greater than the thermal speed $\mathrm{v}_{th,D} \simeq 0.32 C_s$ and $\mathrm{v}_{th,T} \simeq 0.26 C_s$. Therefore, the linear ion Landau damping is negligible as well. On the other hand, the nonlinearly generated beat wave (virtual sound wave) is characterized by much lower phase velocity $\omega''/k''_\parallel \simeq \omega'' q R$ [20, 21]. Consequently its resonant interaction with bulk ions can be considerable and stronger for D with higher thermal speed than for T. This may be the reason why $Q_D > Q_T$ and $\Gamma_D > \Gamma_T$ as observed in the nonlinear simulation and is consistent with our speculation of the ion Compton scattering (nonlinear ion Landau damping) playing the dominant role in

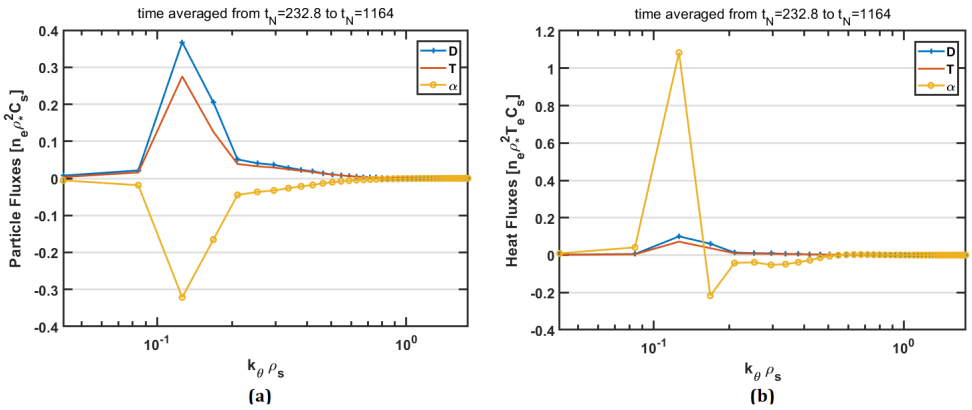

Figure 4: Time averaged (a) particle fluxes and (b) heat fluxes summed over k_r from nonlinear GKW simulations.

nonlinear saturation. It is worthwhile to recall that the bulk plasma transport due to ITG-TEM turbulence in positive shear plasmas gets reduced in the presence of the fast ion [24, 25]. Meanwhile, this work suggests that the bulk ion transport may increase due to the fast ion driven new instability in the RS plasmas.

Fig. 4 shows the time averaged particle fluxes and heat fluxes as functions of k_θ summed over k_r respectively. Both particle and heat fluxes are carried mostly by long wavelength modes and the dominant mode is $k_\theta \rho_s = 0.1263$. An interesting point is that heat flux of α particles is outward for $k_\theta \rho_s < 0.1263$ while inward for $k_\theta \rho_s > 0.1263$.

4. Conclusion

We have studied the nonlinear behavior of turbulence and transport caused by the fast ion precession driven drift instability in RS plasmas using the GKW code. Considerable transport rates observed from simulations indicates potential relevance of this instability in burning plasmas with reversed shear. k_θ-spectrum of saturated fluctuation and difference between transport rate of D and T working gas suggest that ion Compton scattering of bulk ions is a prime candidate for the dominant nonlinear saturation mechanism. Through this mechanism, some EP kinetic energy gets eventually transferred to the main ions. Ion Compton scattering of high mode number

Toroidal Alfvén Eigenmodes (TAE) [26, 27] has been considered as a candidate for alpha-channeling previously [28] and associated modeling studies are being pursued [29]. Possibility of alpha-channeling via the new instability needs to be examined in the future. Heat flux of the fast ions evolves slowly in time well after other quantities reach steady state. Understanding of this property will require further investigation in the future.

CRediT authorship contribution statement

B. J. Kang: Data analysis, assisting GKW simulation, writing formulation and simulation parts of the manuscript.
C. Angioni: Leading GKW simulation, data analysis.
T. S. Hahm: Conceptualization, writing physics interpretation part of the manuscript.

Declaration of competing interest

The authors declare that they have no known competing financial interests or personal relationships that could have appeared to influence the work reported in this paper.

Acknowledgements

T. S. Hahm acknowledges useful discussion with L. Chen, G. J. Choi, W. Heidbrink, Y. Kishimoto, Z. Lin and F. Zonca. The numerical calculations have been performed on the supercomputer Cobra of the Max Planck Computing and Data Facility. This research was supported by Basic Science Research Program through the National Research Foundation of Korea(NRF) funded by the Ministry of Education(NRF-2018R1D1A1A02047428).

Appendix A. Turbulence driven particle fluxes

There has been a sign error in the previous derivation of the quasi-linear particle flux. The minus sign in the first line of Eq. (38) in Ref. [10] should be removed. Then, Eqs. (38) and (39) in Ref. 10 should be modified as

$$\Gamma_{f,\vec{k}} = \frac{k_\theta}{B}\left\langle \Re\left\{ i \int_t d^3\mathrm{v} J_0 \delta g_{f,\vec{k}} \delta\phi^*_{\vec{k}} \right\} \right\rangle \tag{A.1}$$

$$= -2\sqrt{2\pi\epsilon}\frac{Z_f^2|e|^2\langle|\delta\phi_{\vec{k}}|^2\rangle}{T_f^2}n_{f0}\omega_{*e}R$$
$$\times\Big\langle\frac{1}{G(\hat{s},\kappa)}\sqrt{\hat{E}_{0r}(\hat{s},\kappa)}e^{-\hat{E}_{0r}(\hat{s},\kappa)}J_0^2(\sqrt{2b_f\hat{E}_{0r}})$$
$$\times\Big[1-\frac{\omega_{*f}}{\omega_{*e}}\Big\{1+\eta_f\Big(\hat{E}_{0r}(\hat{s},\kappa)-\frac{3}{2}\Big)\Big\}\Big]\Big\rangle_\kappa$$
$$= -\frac{1}{Z_f}\frac{\gamma_{lin}}{\omega_{*e}}k_\theta\rho_s C_s\frac{|e|^2\langle|\delta\phi_{\vec{k}}|^2\rangle}{T_e^2}n_{e0},$$

and

$$\Gamma_i = \langle\delta n_i\delta \mathrm{v}_r\rangle = \langle(\delta n_e - Z_f\delta n_f)\delta \mathrm{v}_r\rangle = -Z_f\Gamma_f \tag{A.2}$$
$$= \sum_{\vec{k}}\frac{\gamma_{lin}}{\omega_{*e}}k_\theta\rho_s C_s\frac{|e|^2\langle|\delta\phi_{\vec{k}}|^2\rangle}{T_e^2}n_{e0}$$

Various notations are defined in Ref. [10]. Therefore the direction of particle fluxes also should be modified. When the instability occurs, we obtain $\Gamma_f < 0$ and $\Gamma_i > 0$ within the assumption of adiabatic electron reponse leading to no electron particle flux. Extended studies including the non adiabatic electron response is necessary to address the implication of this new instability on the direction of particle fluxes.

References

[1] C. Kessel, J. Manickam, G. Rewoldt, and W. M. Tang, Physical Review Letters 72, 1212 (1994).

[2] T. Ozeki, M. Azumi, T. Tsunematsu, K. Tani, M. Yagi, and S. Tokuda, Plasma physics and Controlled Nuclear Fusion Research(Proc. 14th Int. Conf. Wurzburg), Vol.2, IAEA, Vienna (1995).

[3] A. D. Turnbull, T. S. Taylor, Y. R. Lin-Liu, and H. St. John, Physical Review Letters 74, 718 (1995).

[4] L. Chen and F. Zonca, Review of Modern Physics 88, 015008 (2016).

[5] C. Angioni and A. G. Peeters, Physics of Plasmas 15, 052307 (2008).

[6] W. Zhang, Z. Lin and L. Chen, Physical Review Letters 101, 095001 (2008).

[7] S. M. Yang, C. Angioni, T. S. Hahm, D. H. Na and Y. S. Na, Physics of Plasmas 25, 122305 (2018).

[8] M. N. Rosenbluth and F. L. Hinton, Nuclear Fusion 36, 55 (1996).

[9] Y. W. Cho and T. S. Hahm, Nuclear Fusion 59, 066026 (2019).

[10] B. J. Kang and T. S. Hahm, Physics of Plasmas 26, 042501 (2019).

[11] B. J. Kang, Y. J. Kim, C. Angioni and T. S. Hahm, Physics of Plasmas 27, 072510 (2020).

[12] A. G. Peeters, Y. Camenen, F. J. Casson, W. A. Hornsby, A. P. Snodin, D. Strintzi, and G. Szepesi, Computer Physics Communications 180(12), 2650 (2009).

[13] E. A. Frieman and Liu Chen, Physics of Fluids 25, 502 (1982).

[14] T. S. Hahm, Physics of Fluids 31, 2670 (1988).

[15] F. Y. Gang and P. H. Diamond, Physics of Fluids B: Plasma Physics 2, 2976 (1990).

[16] B. H. Fong and T. S. Hahm, Physics of Plasmas 6, 188 (1999).

[17] R. V. Budny and JET Contributors, Nuclear Fusion 58, 096011 (2018).

[18] H. L. Berk, D. N. Borba, B. N. Breizman, S. D. Pinches and S. E. Sharapov, Physical Review Letters 87, 185002 (2001).

[19] H. Kimura, Y. Kusama, M. Saigusa, G. J. Kramer, K. Tobita, M. Nemoto, T. Kondoh, T. Nishitani, O. Da Costa, T. Ozeki, T. Oikawa, S. Moriyama, A. Morioka, G. Y. Fu, C. Z. Cheng and V. I. Afanas'ev, Nuclear Fusion 38, 1303 (1998).

[20] T. S. Hahm and W. M. Tang, Physic of Fluids B 3(4), 989 (1991).

[21] L. Chen, R. L. Berger, J. G. Lominadze, M. N. Rosenbluth and P. H. Rutherford, Physical Review Letters 39, 754 (1977).

[22] Y. Kosuga, P. H. Diamond, G. Dif-Pradalier and Ö. D. Gürcan, Physics of Plasmas 21, 055701 (2014).

[23] Y. Kosuga, S.-I. Itoh, P. H. Diamond, K. Itoh and M. Lesur, Physics of Plasmas 21, 102303 (2014).

[24] J. Citrin, F. Jenko, P. Mantica, D. Told, C. Bourdelle, J. Garcia, J. W. Haverkort, G. M. D. Hogeweji, T. Johnson and M. J. Pueschel, Physical Review Letters 111, 155001 (2013).

[25] J. Garcia, C. Challis, J. Citrin, H. Doerk, G. Giruzzi, T. GÖrler, F. Jenko, P. Magnet and JET Contributors, Nuclear Fusion 55, 053007 (2015).

[26] T. S. Hahm and Liu Chen, Physical Review Letters 74, 266 (1995).

[27] Z. Qiu, L. Chen and F. Zonca, Nuclear Fusion 59, 066024 (2019).

[28] T. S. Hahm, Plasma Science and Technology 17, 534 (2015).

[29] J. M. Seo, Y. S. Na and T. S. Hahm, submitted to Nuclear Fusion (2021).